

Li_{0.44}MnO₂: an intercalation electrode with a tunnel structure and excellent cyclability

A. Robert Armstrong, Haitao Huang, Richard A. Jennings and Peter G. Bruce*

Centre for Advanced Materials, School of Chemistry, University of St. Andrews, St. Andrews, Fife, UK KY169ST

Li_{0.44}MnO₂ possesses a complex tunnel structure composed of sheets of edge-sharing MnO₆ octahedra and columns of edge-sharing MnO₅ square pyramids both lying parallel to the *c* axis of the orthorhombic unit cell (space group *Pbam*). The sheets and columns corner share thus defining two types of tunnels. The smaller of these contains one Li⁺ ion site and the larger two pairs of Li⁺ sites. There are no less than five crystallographically distinct Mn sites. The lithium content of the host has been varied by chemical and electrochemical intercalation/deintercalation over the range Li_{*x*}MnO₂; 0.25 < *x* < 0.63. The associated change in the lithium site occupancies has been determined by a combination of powder neutron diffraction and electrochemical measurements. The structure demonstrates a remarkable ability to cycle lithium with no perceptible loss of capacity when cycled over the range 2.8–3.6 V vs. Li⁺(1 M)/Li, at 0.5 mA cm⁻² corresponding to a capacity of 85–90 mA h g⁻¹.

Production of the first generation of rechargeable lithium batteries is growing rapidly. Such cells are setting new standards of performance in many consumer electronic products. In particular they represent a leap forward in energy density compared with conventional systems, *e.g.* nickel–cadmium or nickel–metal–hydride.¹ Despite the success of the rechargeable lithium battery, use of the intercalation compound LiCoO₂ as the positive electrode presents several problems, not the least of which are the relatively high cost and toxicity of this material.^{1,2} The spinel intercalation electrode, LiMn₂O₄, is much cheaper and less toxic than LiCoO₂. It has been developed over 10 years.^{3–9} Nippon Moli recently announced a second generation rechargeable lithium battery in which LiCoO₂ is replaced by the spinel.¹⁰ Despite the somewhat lower practical capacity to store charge (110 mA h g⁻¹ for LiMn₂O₄ as opposed to 130 mA h g⁻¹ for LiCoO₂) the much lowered cost and toxicity of the spinel electrode make its use attractive. Cost is a crucial parameter, particularly in the context of designing larger scale batteries for electric vehicle applications. Recently we reported the synthesis of a layered compound LiMnO₂ with a structure analogous to that of LiCoO₂.¹¹ The initial capacity is high, >200 mA h g⁻¹ even at the high current density of 0.5 mA cm⁻², although this does fade on cycling.^{12,13}

One of the major challenges in the development of improved rechargeable lithium batteries is the need to find new metal oxide intercalation hosts for lithium that offer high performance as positive electrodes. Such materials must exhibit a high voltage *vs.* the Li⁺/Li couple, a high capacity to cycle lithium and excellent retention of this capacity on cycling at high rate. The choice of metal oxides which can fulfil all the criteria is limited.³ We are constrained to metal oxides based mainly on the later members of the first row transition series. The importance of cost and toxicity in particular, sustains our interest in lithium manganese oxides. Since the scope to change the composition of the intercalation host is limited we must exercise ingenuity in the design of new structures that may offer better performance than the existing lithium manganese oxide phases. We wish to move from the layered and close packed structures, which have received so much attention in recent years, exploring a wider range of structure types.

Sodium, being larger than lithium, often stabilises manganese oxides with different structures.¹¹ One such phase is Na_{0.44}MnO₂ which exhibits a tunnel structure. Some work has been reported in the literature concerning this compound.^{14,15}

The focus has been mainly on the sodium phase or compositions in which some of the sodium has been replaced by lithium. Here we report an electrochemical and structural study of the fully exchanged Li_{0.44}MnO₂. Galvanostatic cycling and slow sweep cyclic voltammetry are combined with structural studies using powder neutron diffraction, the latter is important as a means of obtaining accurate information on the lithium distribution within the tunnels permitting in turn a deeper understanding of the electrochemical performance.

Experimental

The synthesis of Li_{0.44}MnO₂ was achieved *via* preparation of Na_{0.44}MnO₂ followed by ion exchange to replace the sodium by lithium. The parent compound Na_{0.44}MnO₂ (Na₄Mn₉O₁₈) was synthesised by a conventional solid state route in which a mixture of Na₂CO₃ and Mn₂O₃ in the stoichiometric ratio 1:2 was fired at 800 °C for 15–24 h in air. A slight excess of sodium was required to produce a single phase product. Previous syntheses, which did not employ an excess, resulted in the formation of some Mn₂O₃.¹⁵ Phase purity was verified by powder X-ray diffraction using a Philips X'Pert PW3020 diffractometer operating with Bragg–Brentano geometry and Cu-K α radiation. An analysing monochromator was employed to reduce fluorescence at the detector. Initial ion exchange experiments employed the same route as was used in the preparation of layered LiMnO₂, reflux in *n*-hexanol with an excess of LiBr.^{11,12} This approach gave incomplete exchange, suggesting that more rigorous conditions were necessary. Two different melts were investigated: a eutectic mixture of LiCl/KCl (40.5/59.5 mol%) at 380 °C, and a eutectic mixture of LiNO₃/LiCl (88/12 mol%) at 260–275 °C. The former yielded a single phase product with the spinel structure whilst the latter gave the desired Na₄Mn₉O₁₈ structure. Na_{0.44}MnO₂ was mixed with an appropriate amount of the ion exchange medium (5–10-fold Li excess) and fired at 260–275 °C. On cooling, the solidified melt was dissolved in ethanol and the product filtered, washed and dried. Once again phase purity was verified using powder X-ray diffraction.

Materials with different lithium contents were prepared by chemical oxidation and reduction. Oxidised materials were synthesised by reaction with a solution of bromine in acetonitrile at room temperature. Lithium insertion was performed by refluxing in a solution of LiI in acetonitrile. In view of the

photosensitivity of lithium iodide the reaction vessel was covered in aluminium foil.

The structures of these materials were characterised using neutron diffraction. Time-of-flight powder neutron diffraction data were collected on the POLARIS high-intensity, medium-resolution instrument at ISIS, Rutherford Appleton Laboratory.¹⁶ The structures were refined by the Rietveld method using the program TF14LS based on the Cambridge Crystallographic Subroutine Library (CCSL).^{17,18} Neutron scattering lengths of -0.19 , -0.3703 and 0.5803 (all $\times 10^{-12}$ cm) were assigned to Li, Mn and O respectively.¹⁹

Electrochemical cells were prepared containing working electrodes consisting of $\text{Li}_{0.44}\text{MnO}_2$ /carbon black/polytetrafluoroethylene (PTFE) in the weight ratios 80:13:7. These were dry mixed and pressed onto aluminium grids. The electrolyte consisted of a 1 M solution of battery grade LiAsF_6 (Lithco) dissolved in propylene carbonate (Aldrich) and the counter and reference electrodes were made of lithium metal. The solvent was distilled as described elsewhere.⁴ The electrochemical experiments were controlled by a Biologic Macpile multichannel instrument.

Results and Discussion

Electrode performance

The load curve for $\text{Li}_{0.44}\text{MnO}_2$, collected at a constant current density of $10 \mu\text{A cm}^{-2}$ and between potential limits of 2.5 and 3.7 V, is shown in Fig. 1. These data correspond to the first cycle which commences with discharge from 3.3 V. The separation of charge and discharge curves within the range 3.3–2.5 V is small and non-existent on the scale of Fig. 1. We may conclude that there is negligible hysteresis between charge and discharge when cycling lithium within the tunnel structure of $\text{Li}_{0.44}\text{MnO}_2$. The cyclic voltammogram for this electrode collected at a sweep rate of $10 \mu\text{V s}^{-1}$ and within the range 2–3.8 V is shown in Fig. 2. As expected there is good correspondence between the data in Fig. 1 and 2 although the different electrochemical processes are more clearly resolved in the cyclic voltammograms. Three well separated redox processes are evident in Fig. 2. Closer inspection of the process with redox peaks in the region of 3.1 V indicates that this can be resolved into two processes, the second being apparent as a shoulder on the high voltage side of the first. The redox reaction at the lowest voltage is the least reversible with the reduction peak being severely elongated along the voltage axis. Although the general features of the cyclic voltammogram are retained on cycling, some variation may be noted particularly at the lower voltages. The reduction between 2 and 2.3 V becomes less evident and the intensity of the associated oxidation peak at around 2.8 V diminishes significantly. The results of cyclic voltammograms carried out over the more

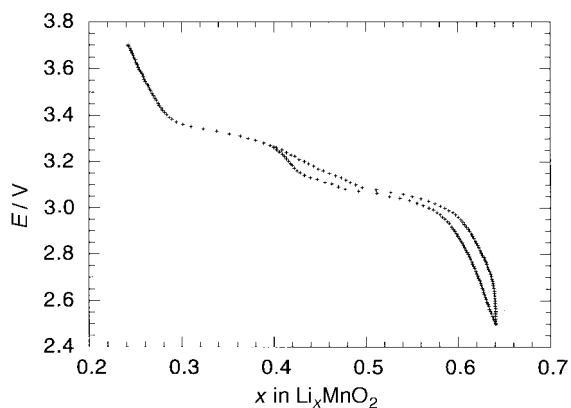


Fig. 1 Variation of electrode potential with composition for Li_xMnO_2 at a current density of $10 \mu\text{A cm}^{-2}$

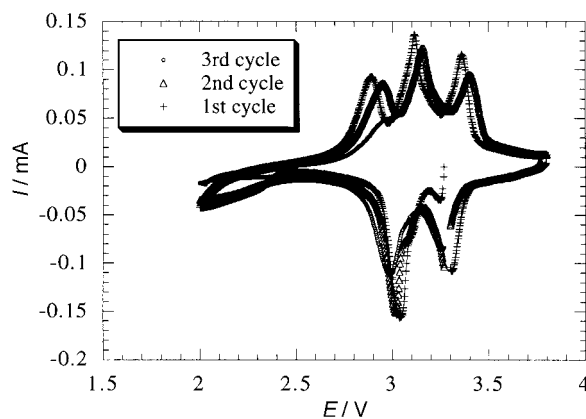


Fig. 2 Cyclic voltammogram for Li_xMnO_2 at a sweep rate of $10 \mu\text{V s}^{-1}$ between 2.0 and 3.8 V

restricted potential range of 2.6–3.6 V are presented in Fig. 3. By avoiding the lowest voltage process, retention of charge on cycling is now very good. As discussed later it may be more appropriate to describe the composition of the material after ion exchange as $\text{Li}_{0.40}\text{MnO}_2$ rather than $\text{Li}_{0.44}\text{MnO}_2$, then the quantity of charge passed on the first reduction (Fig. 3) corresponds to a composition of $\text{Li}_{0.63}\text{MnO}_2$ at 2.6 V and this agrees well with the load curve (Fig. 1). The maximum lithium content that may be accommodated in the tunnel structure corresponds to $\text{Li}_{0.67}\text{MnO}_2$ (see later) implying that the host reaches almost full intercalation at 2.6 V. Therefore the reduction at lower voltage in Fig. 2 probably corresponds to decomposition of the tunnel compound consistent with the irreversible nature of this process. Oxidation to 3.6 V corresponds to a composition of $\text{Li}_{0.32}\text{MnO}_2$. Neither electrochemical oxidation to higher voltages (up to 4.3 V) nor chemical oxidation with bromine can remove all the lithium. The minimum lithium content that can be achieved is approximately $\text{Li}_{0.25}\text{MnO}_2$. This is in accord with the previously reported studies on $\text{Na}_{0.44}\text{MnO}_2$ which also demonstrated the difficulty of removing all the guest ions.¹⁵

A more extensive investigation of lithium cycling is presented in Fig. 4. Cycling was carried out at a current density of 0.5 mA cm^{-2} and over the potential range 2.8–3.6 V. The most remarkable feature is the lack of capacity fade even after 100 cycles. There is no perceptible loss of capacity with increasing cycle number, any change is confined to fluctuations between cycles. Furthermore the charge and discharge curves are superimposed even at this high current density. The capacity is limited to $85\text{--}90 \text{ mA h g}^{-1}$, which places it somewhat below

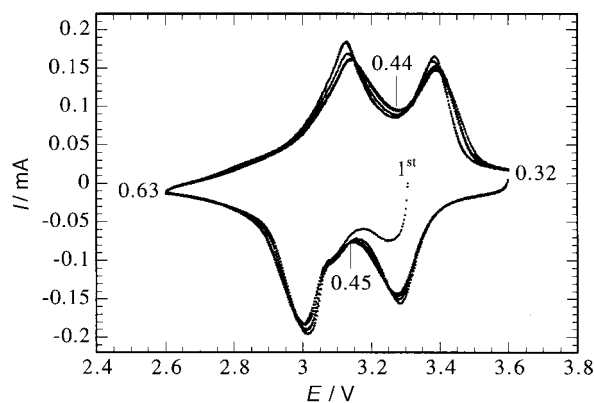


Fig. 3 Cyclic voltammogram for Li_xMnO_2 at a sweep rate of $10 \mu\text{V s}^{-1}$ between 2.6 and 3.6 V. Numbers given on the plot refer to values of x estimated from the charge passed.

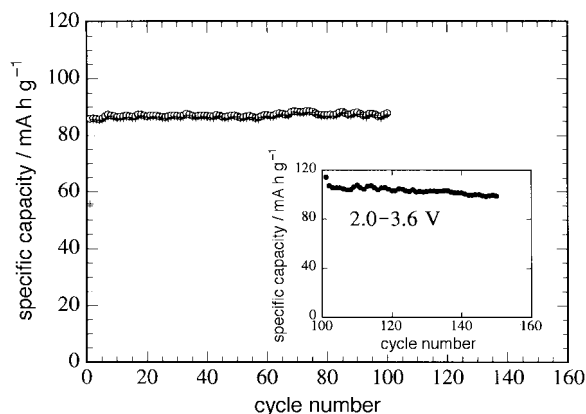


Fig. 4 Variation in specific capacity (○, charge; +, discharge) as a function of cycle number at a current density of 0.5 mA cm^{-2} between voltage limits of 2.8 and 3.6 V vs. Li^+/Li . Inset shows effect on capacity of extending voltage limits to 2.0–3.6 V.

the LiMn_2O_4 spinel at 110 mA h g^{-1} and the average voltage of the tunnel compound (3.2 V) is also less than can be obtained from the spinel on the 4 V plateau. The voltage of the tunnel structure is too low for some applications in rocking chair cells. Nevertheless, the capacity retention is much better than can be obtained from the spinel material. Comparing the tunnel structure with other low cost, low toxicity contenders, it is worth considering two other spinel based manganese oxides, $\text{Li}_2\text{Mn}_4\text{O}_9$ and $\text{Li}_4\text{Mn}_5\text{O}_{12}$.²⁰ Both materials cycle at a somewhat lower voltage than the tunnel structure (*i.e.* 3 V) but have higher initial capacities of around 130 mA h g^{-1} . It is difficult to assess the capacity fade of these materials as cycling data reported in the literature extends only to some 12 cycles.²⁰ It appears that capacity retention is good in the case of these 3 V spinel compounds, although close inspection of the reported cycling curves suggests it is somewhat inferior compared with the tunnel compound.

Whereas for a number of applications in electronic devices the ability to charge and discharge cells over several hundred cycles may be sufficient, there is no doubt that the future development of rechargeable lithium batteries will impose far greater demands on the cyclability. For certain consumer applications and particularly for the application of such batteries in electric vehicles, the ability to cycle cells 1000 times while retaining much of the original capacity will become an imperative. In this context the present generation of materials including the LiMn_2O_4 spinel cannot match the required performance. It is therefore critically important to search for new structures that better support cycling of the guest lithium ions. The evidence presented here indicates that tunnel structures may offer a promising way forward in this regard. Various factors have been proposed to explain the loss of capacity on cycling for intercalation electrodes in general. They have included, dissolution of the electrode at high or low states of charge (*i.e.* high or low voltage),⁸ and first order phase transitions during intercalation/deintercalation the latter associated with an abrupt volume change, leading to loss of interparticle contact and hence isolation of regions in the electrode. We have reported direct evidence for the latter in the case of the 3 V spinel LiMn_2O_4 .¹² For the tunnel compound X-ray diffraction gives no evidence of a two phase reaction. This, along with a modest volume change of 4% between $\text{Li}_{0.25}\text{MnO}_2$ and $\text{Li}_{0.65}\text{MnO}_2$, may, at least in part, be responsible for the excellent capacity retention of the compound.

The voltage range chosen for the cycling data in Fig. 4 avoids the lowest voltage process in the cyclic voltammogram of Fig. 3. By extending the voltage range so that cycling was carried out from 3.6 to 2.0 V the additional capacity associated

with this low voltage process may be obtained but at the expense of capacity retention (see inset in Fig. 4). Any extension of the potential range beyond 2.8 to 3.6 V that is sufficient to increase significantly the initial capacity also increases the capacity fade.

The structure of Li_xMnO_2

Six compositions were prepared by solid state reaction followed by chemical intercalation/deintercalation, with nominal compositions $\text{Li}_{0.25}\text{MnO}_2$, $\text{Li}_{0.32}\text{MnO}_2$, $\text{Li}_{0.40}\text{MnO}_2$, $\text{Li}_{0.45}\text{MnO}_2$, $\text{Li}_{0.55}\text{MnO}_2$ and $\text{Li}_{0.65}\text{MnO}_2$. The powder X-ray diffraction patterns for each composition could be indexed on the structure of the analogous $\text{Na}_4\text{Mn}_4\text{Ti}_5\text{O}_{18}$ (space group $Pb3m$)²¹ and this structure was used as a basis for the Rietveld refinements of neutron diffraction data for three of the compositions: $\text{Li}_{0.25}\text{MnO}_2$, $\text{Li}_{0.40}\text{MnO}_2$ and $\text{Li}_{0.65}\text{MnO}_2$. The crystallographic data for these refinements are presented in Table 1 and the fitted profile for the $\text{Li}_{0.25}\text{MnO}_2$ compound is shown in Fig. 5. The single crystal structure of the $\text{Na}_4\text{Mn}_4\text{Ti}_5\text{O}_{18}$ has been used previously as a model for the structure of $\text{Na}_{0.44}\text{MnO}_2$.²²

The refined structure of $\text{Li}_{0.40}\text{MnO}_2$ is shown in Fig. 6. Only minor variations occur in the Mn–O framework on varying the lithium content therefore the model shown in Fig. 6 is representative of the structure over the entire composition range, the main variation being confined to changes in lithium occupancy of three crystallographically distinct sites. The tunnels present in this structure are clearly evident in the

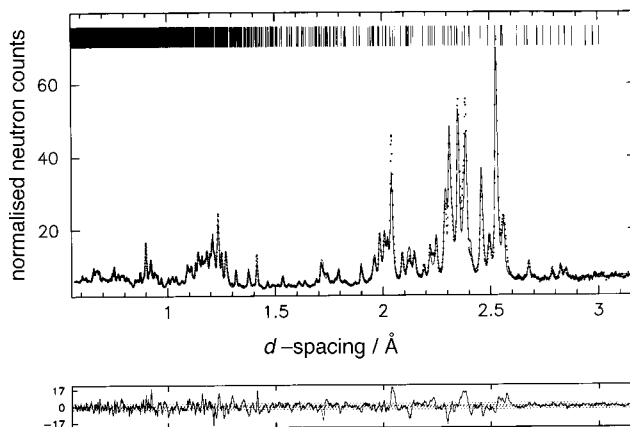


Fig. 5 Observed (dots) and calculated (solid line) neutron diffraction profiles for $\text{Li}_{0.25}\text{MnO}_2$. The lower plot shows the difference/estimated standard deviation.

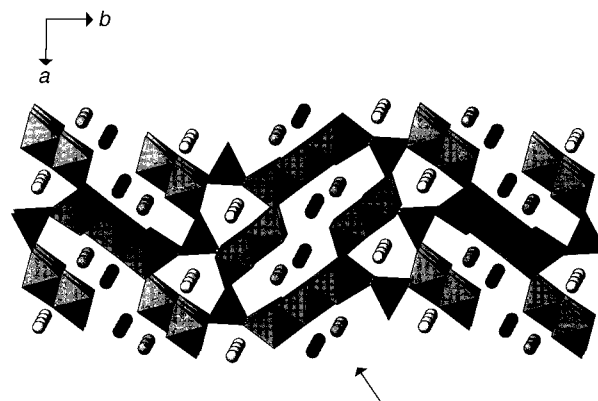


Fig. 6 Structure of $\text{Li}_{0.4}\text{MnO}_2$ looking down the c axis showing MnO_x polyhedra. Li(1) (in the small tunnels, pale circles), Li(2) (ends of S-shaped tunnels), medium circles, Li(3) (middle of S-shaped tunnels), dark circles.

Table 1 Atomic coordinates, thermal parameters and occupancy factors for $\text{Li}_{0.4}\text{MnO}_2$ and structural parameters for $\text{Li}_x\text{MnO}_2^a$

atom	Wyckoff symbol	x/a	y/b	z/c	B_{iso}	occupancy
Li(1)	4g	0.144(3)	0.1916(13)	0.0	2.0(-)	0.84(7)
Li(2)	4h	0.187(7)	0.422(2)	0.5	2.0(-)	0.46(7)
Li(3)	4g	0.177(6)	-0.017(2)	0.0	2.0(-)	0.49(7)
Mn(1)	2c	0.0	0.5	0.0	0.7(2)	
Mn(2)	4h	0.3215(9)	0.3110(4)	0.5	0.14(11)	
Mn(3)	4g	-0.0066(13)	0.1063(4)	0.0	0.43(12)	
Mn(4)	4g	-0.0182(10)	0.3087(4)	0.0	0.69(14)	
Mn(5)	4h	0.3387(12)	0.0803(4)	0.5	0.9(2)	
O(1)	4h	0.3526(8)	0.0051(2)	0.5	0.16(7)	
O(2)	4g	0.1986(7)	0.0827(3)	0.0	0.59(9)	
O(3)	4h	0.0173(9)	0.1573(3)	0.5	1.47(12)	
O(4)	4h	0.3556(9)	0.1663(3)	0.5	1.44(12)	
O(5)	4h	0.1113(7)	0.2882(2)	0.5	0.92(11)	
O(6)	4g	0.3572(8)	0.2656(3)	0.0	0.54(8)	
O(7)	4g	0.2827(7)	0.3633(2)	0.0	0.65(10)	
O(8)	4g	0.4864(7)	0.0816(2)	0.0	0.51(9)	
O(9)	4h	0.4488(12)	0.4398(4)	0.5	2.1(2)	

^a $\text{Li}_{0.40}\text{MnO}_2$; orthorhombic, space group *Pbam*, $a=8.9316(2)$, $b=24.4350(5)$, $c=2.83072(5)$ Å, $R_{\text{exp}}=0.9\%$, $R_{\text{wp}}=4.4\%$, $R_p=7.1\%$. $\text{Li}_{0.25}\text{MnO}_2$; $a=8.91015(13)$, $b=24.0725(4)$, $c=2.82588(4)$ Å, $R_{\text{exp}}=0.9\%$, $R_{\text{wp}}=4.0\%$, $R_p=6.2\%$. Li(1) occupancy=0.67(5), Li(2) vacant, Li(3) occupancy=0.47(6). $\text{Li}_{0.65}\text{MnO}_2$; $a=8.9435(2)$, $b=25.0485(6)$, $c=2.82393(6)$ Å, $R_{\text{exp}}=0.9\%$, $R_{\text{wp}}=4.6\%$, $R_p=7.2\%$. Li(1) occupancy=0.85(7), Li(2) occupancy=1, Li(3) occupancy=1.

projection in Fig. 6. The Mn–O framework consists of two types of sheets formed from MnO_6 octahedra sharing common edges and lying along the c -axis, as well as chains of edge sharing MnO_5 square pyramids which also lie along c . The sheets and chains are linked together by corner sharing thus forming two distinct tunnels parallel to c ; the smaller of these is defined by four MnO_6 octahedra and two MnO_5 square pyramids, whereas the larger tunnels are S-shaped and are defined by ten MnO_6 octahedra and two MnO_5 square pyramids. Three crystallographically distinct Li^+ sites are present within these tunnels, one, Li(1), in the smaller tunnels and two, Li(2) and Li(3), in the larger S-shaped tunnels. The Li sites are arranged in columns along c and symmetry generates a further column of Li(2) and Li(3) sites within each S-shaped tunnel, Fig. 6. In the case of $\text{Li}_{0.40}\text{MnO}_2$ the site located in the small tunnels exhibits an occupancy of 0.84(7), whereas the sites in the S-shaped tunnels are both one-half occupied within one esd. The sample composition refines to $\text{Li}_{0.40(5)}\text{MnO}_2$. The ideal composition $\text{Li}_{0.44}\text{MnO}_2$ (in which the large tunnel sites are exactly half full and the Li(1) site is fully occupied) is within one esd of the 0.40 composition. For consistency with the other refinements and with deference to the possibility of slight oxidation in the nitrate melt used for ion exchange, we have elected to describe the composition as 0.40. Given that $\text{Li}_{0.44}\text{MnO}_2$ exhibits half occupancy of the Li(2) and Li(3) sites, coupled with the absence of any evidence from the neutron data supporting long range ordering of lithium, it is likely that the Li^+ ions order over the short range within each tunnel. The tendency to order is less between sites in neighbouring tunnels given their relative distance compared with the close proximity of Li^+ inside the tunnels. The nature of any ordering will depend on the Li(2)–Li(2) and Li(3)–Li(3) distances along the c -axis (2.8 Å in both cases) as well as the shortest Li(2)–Li(3) (2.4 Å), and the Li(3)–Li(3) (3.3 Å) distance in the ab plane. Although many ordering schemes are possible, two are likely to be particularly favoured energetically, Fig. 7. The short Li(2)–Li(3) distance mitigates against an ordering scheme involving occupancy of alternate sites in the c -direction. The Li(2) and Li(3) sites are displaced one from the other by $0.5c$ so that such ordering cannot avoid the short Li(2)–Li(3) distances. Fig. 7(a) describes alternate occupancy along c ; there is a single Li(2)–Li(3) distance for each Li^+ ion. In contrast full occupancy of one column of Li(2) sites and the most distant column of Li(3) sites as envisaged in Fig. 7(b) involves only one short Li–Li distance along c for

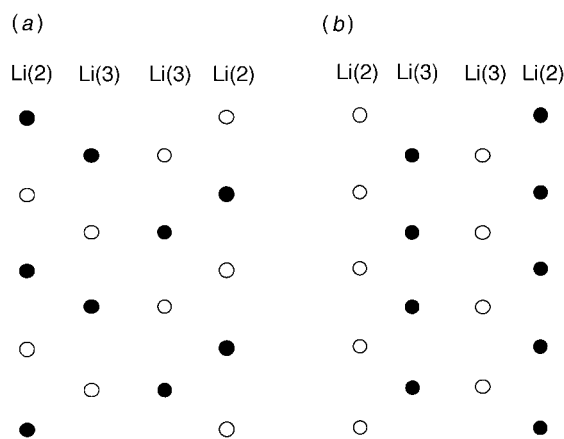


Fig. 7 Schematic representation of two different ordering schemes for Li^+ , viewed from the direction shown by the arrow in Fig. 6 and showing the columns of Li(2) and Li(3) sites along the c -axis. (a) Alternate Li(2) and Li(3) vacancies along c -direction; (b) alternate columns of filled Li(2) and Li(3) sites. [○, vacant Li site; ●, filled Li site]

each lithium. Since this distance is more than the Li(2)–Li(3) distance (2.8 vs. 2.4 Å), scheme (b) (Fig. 7) is more likely to exist.

In the delithiated sample, $\text{Li}_{0.25}\text{MnO}_2$, the Li(2) sites in the S-shaped tunnels are empty but there is no change in the occupancy of the Li(3) sites. There is some evidence of depletion in the lithium content of the Li(1) sites in the smaller tunnels but this change is more minor compared with the changes occurring in the larger tunnels. Considering the fully intercalated sample $\text{Li}_{0.65}\text{MnO}_2$, it is clear from Table 1 that all three lithium sites are essentially fully occupied. Evidently in the case of this intercalation compound the structural chemistry imposes a limit on the maximum lithium content.

Despite the high degree of structural complexity exhibited by this compound the use of neutron diffraction data has permitted establishment of a relatively clear and simple trend in the occupancy of the lithium sites within the tunnels.

Correlating the structure with the electrochemistry

Armed with this detailed structural information it is possible to interpret the intercalation electrochemistry in terms of the

structural changes. Since the features of the electrochemistry are most clearly exhibited in the slow sweep cyclic voltammetry we shall correlate the redox processes highlighted therein with the structural changes. The main interest in this compound is its exceptional capacity retention on cycling, as a result attention will be focused on the processes occurring within the potential range over which high cycling efficiency is obtained *i.e.* the cyclic voltammogram in Fig. 3. Beginning at 3.25 V which corresponds to the composition $\text{Li}_{0.44}\text{MnO}_2$, the oxidation peak at 3.40 V is associated with removal of lithium from the Li(2) sites in the S-shaped tunnels. We know from the structural studies that extraction of lithium to yield $\text{Li}_{0.25}\text{MnO}_2$ involves removing the one-half of the lithium on the Li(2) sites and possibly a smaller amount of lithium from the Li(1) sites. The quantity of charge removed electrochemically is equivalent to extraction of 0.12 lithium atoms per formula unit. Full occupancy of any of the lithium sites corresponds to 0.22 lithiums, hence the charge extracted is in close agreement with removal of the one-half of the lithium on the Li(2) sites. These sites are refilled to an occupancy of one-half during the subsequent reduction at 3.3 V. The two closely spaced reduction processes at 3 and 3.1 V are associated with filling of the remaining half of the Li(2) and Li(3) sites. The change in the lithium content of 0.18 is in good agreement with that predicted for complete occupancy of the Li(2) and Li(3) sites. Two facts are worthy of comment. First, why should changing the Li(2) site occupancy from 0 to 0.5 and from 0.5 to 1 occur with a difference of energy corresponding to 300 mV? The answer probably lies in the discussion of short range order (in the previous section). Insertion of Li into the Li(2) site beyond an occupancy of one-half involves filling the second column of Li(2) sites and this introduces the short Li(2)–Li(3) contacts that were avoided in the ordering scheme for $\text{Li}_{0.44}\text{MnO}_2$. As a consequence the energy of Li^+ ions in the second Li(2) column is greater. We have assumed that the reduction below 3.2 V involves filling the Li(2) and Li(3) sites beyond one-half occupancy. In the case of both sites short Li(2)–Li(3) contacts are introduced which may explain the similarity in energy of these processes. It is important to note in this context that the two closely spaced reductions do not correspond respectively to filling the Li(2) and Li(3) sites. This would require the peaks to be of equal size. There are no less than five crystallographically distinct Mn sites. Bond valence calculations are consistent with an invariant oxidation state of 3+ for Mn on the square pyramidal site, giving values of 2.94, 3.08 and 2.93 for $\text{Li}_{0.25}\text{MnO}_2$, $\text{Li}_{0.40}\text{MnO}_2$ and $\text{Li}_{0.65}\text{MnO}_2$ respectively. Similar calculations for the other sites indicate that the valences change but the complexity of the system makes such calculations too imprecise to merit detailed analysis. However all appear to be involved in the redox processes and given their inequivalence the contribution to the energetics

of intercalation from these will be different. We speculate that the resolution of the reduction current into two processes below 3.2 V may arise from a switch of the active Mn sites

It is clear that $\text{Li}_{0.44}\text{MnO}_2$ is a complex structure and exhibits complex intercalation chemistry that can nevertheless be understood in some detail by combining electrochemical and structural techniques. While this tunnel structure may not in itself be of immediate use in applications it does possess an important and attractive capacity retention on cycling demonstrating the potential utility of tunnel structures for future applications as electrodes in rechargeable lithium batteries.

P.G.B. is indebted to the EPSRC and the EU for financial support. We thank the EPSRC for the provision of neutron beam facilities, and Colin Morton for synthesising some of the compositions.

References

- 1 P. G. Bruce, *Philos. Trans. R. Soc. London, Ser. A*, 1996, **354**, 1577.
- 2 Y. Gao and J. R. Dahn, *J. Electrochem. Soc.*, 1996, **143**, 100.
- 3 P. G. Bruce, *Chem. Commun.*, 1997, 1817.
- 4 H. Huang and P. G. Bruce, *J. Electrochem. Soc.*, 1994, **141**, L106.
- 5 H. Huang and P. G. Bruce, *J. Power Sources*, 1995, **54**, 52.
- 6 M. M. Thackeray, W. I. F. David, P. G. Bruce and J. B. Goodenough, *Mater. Res. Bull.*, 1983, **18**, 461.
- 7 M. M. Thackeray, P. J. Johnson, L. A. de Picciotto, W. I. F. David, P. G. Bruce and J. B. Goodenough, *Mater. Res. Bull.*, 1984, **19**, 179.
- 8 R. J. Gummow, A. de Kock and M. M. Thackeray, *Solid State Ionics*, 1994, **69**, 59.
- 9 J. M. Tarascon, W. R. McKinnon, F. Coowar, T. N. Bowmer, G. Amatucci and D. Guyomard, *J. Electrochem. Soc.*, 1994, **141**, 1421.
- 10 Japan Electronics, March 6th, 1996.
- 11 A. R. Armstrong and P. G. Bruce, *Nature (London)*, 1996, **381**, 499.
- 12 P. G. Bruce, A. R. Armstrong and H. Huang, *J. Power Sources*, in press.
- 13 C. Delmas and F. Capitaine, *J. Power Sources*, in press.
- 14 M. M. Doeff, M. Y. Peng, Y. Ma and L. C. De Jonghe, *J. Electrochem. Soc.*, 1994, **141**, L145.
- 15 M. Doeff, T. J. Richardson and L. Kepley, *J. Electrochem. Soc.*, 1996, **143**, 2507.
- 16 R. I. Smith, S. Hull and A. R. Armstrong, *Mater. Sci. Forum*, 1994, **166–169**, 251.
- 17 J. C. Matthewman, P. Thompson and P. J. Brown, *J. Appl. Crystallogr.*, 1982, **15**, 167.
- 18 P. J. Brown and J. C. Matthewman, Rutherford Appleton Laboratory Report, 1987, RAL-87-010.
- 19 V. F. Sears, *Neutron News*, 1992, **3**, 26.
- 20 M. M. Thackeray, A. de Kock, M. H. Roussouw, D. Liles, R. Bittihn and D. Hoge, *J. Electrochem. Soc.*, 1992, **139**, 363.
- 21 W. G. Mumme, *Acta Crystallogr., Sect. B*, 1968, **24**, 1114.
- 22 J.-P. Parant, R. Olazcuaga, M. DeValette, C. Fouassier and P. Hagenmuller, *J. Solid State Chem.*, 1971, **3**, 1.

Paper 7/05099B; Received 16th July, 1997